Preprints of the 21st IFAC World Congress (Virtual)
Berlin, Germany, July 12-17, 2020

Multi-Building Systems Thermal and Energy Management via Geothermal Heat Pump ⋆

Lei Liang * **Xiaotian Wang** ** **Xuan Zhang** ***
Hongbin Sun, *Fellow*, *IEEE* ****

* *Tsinghua-Berkeley Shenzhen Institute, Shenzhen, Guangdong, China (e-mail: liangl18@mails.tsinghua.edu.cn)*
** *Tsinghua-Berkeley Shenzhen Institute, Shenzhen, Guangdong, China (e-mail: xt-wang18@mails.tsinghua.edu.cn)*
*** *Tsinghua-Berkeley Shenzhen Institute, Shenzhen, Guangdong, China (e-mail: xuanzhang@sz.tsinghua.edu.cn)*
**** *Department of Electrical Engineering, Tsinghua University, Beijing, China (e-mail: shb@mail.tsinghua.edu.cn)*

Abstract: With the growing concern on energy consumption, optimization and control of Geothermal Heat Pump (GHP) systems have become a research hotspot, which can help solve the problem of building energy conservation and shortage. The superiority of current control schemes of GHP systems is often reflected on an individual building with a separate GHP system. However, with the development of urban construction and the increase of population density, study on the district/area case in built-up areas deserves more attention. This paper focuses on typical cases of one GHP system serving multiple buildings and the community-level coordination of GHP systems. In particular, we present a high-order thermal dynamic model of radiator pipes combined with a commonly used second-order resistance-capacitance model for radiator heating/cooling. We design controllers to improve the efficiency of heat pumps and the ability to track a given nominal point of electrical power consumption in a distributed way, without sacrificing too much user comfort. Simulation results show that the proposed real-time distributed temperature control schemes are effective.

Keywords: Building automation, temperature control, distributed control, building energy management, geothermal heat pump, optimization.

1. INTRODUCTION

According to International Energy Agency, the energy consumption of the building sector occupies more than a third of the global energy consumption, and results in approximately 40% of greenhouse gas emissions and 70% of electricity use (Amara et al. (2015)). Building energy consumption is imputable mainly to Heating Ventilation and Air Conditioning (HVAC) systems, which account for 50% of energy consumption (Pérez-Lombard et al. (2008)). Improving the efficiency of the HVAC system without sacrificing the user comfort has attracted considerable attention recently as a way to assist in reducing building energy consumption.

Among different HVAC systems, the Geothermal Heat Pump (GHP) system has increased in popularity for heating and cooling due to the advantages of high efficiency, low emission, economy and good performance on the user comfort. As stated in Self et al. (2013), the GHP system can generate $3 \sim 5$kWh heat/cold energy from 1kWh electricity. Besides, gas emission of the GHP system is about 70% less than the electric resistance heating with standard air-conditioning equipment, and 40% less than that of air-source heat pump systems (Tahersima et al. (2011)). Moreover, compared with traditional heating and cooling strategies, the GHP system can save $30 \sim 70\%$ of the operating cost of heating and $20 \sim 50\%$ of cooling for the residents on average, see Informative (2019).

The optimization and control of the GHP systems are particularly important in achieving efficient use of heat pumps and energy saving. Until now, many literature have discussed different control techniques related to radiator systems and radiant floor heating systems with GHP. For floor heating, ON/OFF control (Madani et al. (2011)) and Proportional-Integral-Derivative (PID) control (Afram and Janabi-Sharifi (2016)) can adjust heat flux transmitted through floor to maintain room temperature in a desired range. These conventional controllers can be simply implemented, while they could cause thermal fluctuations and decrease the user comfort. Also, the effect of dead-band is hard to avoid. Advanced controllers, including predictive control (Joe and Karava (2019)) and learning-based control (Al Shibli and Mathew (2019)), can largely improve the performance of the radiant floor

⋆ This work was supported by Tsinghua-Berkeley Shenzhen Institute Research Start-Up Funding and Shenzhen Science and Technology Program (Grant No. KQTD20170810150821146). *Corresponding Author: Xuan Zhang.*

heating systems on energy saving. Nevertheless, for multiple connected zones, the above-mentioned methods have to spend huge costs for modeling, data collection, expert monitoring and deployment. For radiator heating, the optimal control combined with a PID controller can save energy and maintain the user comfort in the building, see Maivel and Kurnitski (2014). Nevertheless, the control plan largely relies on the predicted data and its performance is highly sensitive to uncertainties. Advanced distributed MPC as shown in Wen and Mishra (2018) could realize demand response with fast convergence, while the communication costs are high. The controller could perform well with good prediction on disturbances like outdoor temperature and indoor disturbances. Also, the radiator-related control design with more accurate thermal dynamic models in district/area cases is lacking.

Contribution of the paper. This paper proposes a real-time control plan for thermal and energy management of the community-level GHP systems with radiator heat distribution subsystems. We formulate more accurate and realistic thermal models including a high-order thermal dynamic model for radiator pipes and a second-order resistance-capacitance model for rooms. We consider practical operational constraints and focus on two schemes, one GHP system serving multiple buildings and community-level coordination of multiple GHP systems. By a distributed algorithm, the designed control scheme could track a given nominal point of electrical power consumption with high efficiency and comfort. Also, the controller is easy to scale with simple communication structures and can be implemented without measuring outdoor temperatures and indoor heat disturbances.

2. PRELIMINARIES

2.1 The Operating Principle of a GHP System

The structure of a typical GHP system is demonstrated in Figure 1. It primarily consists of three subsystems: the underground heat exchange subsystem, the heat pump subsystem and the heat distribution subsystem. Pipes with a hydraulic circuit in the heat exchange subsystem are employed to extract thermal energy from the ground or store heat for heating/cooling in the heat pump subsystem. The heat pump subsystem consists of compressors, expansion valves, reversing valves, evaporators and condensers (Omer (2008)). In the heat distribution subsystem, rooms are equipped with radiator systems or floor radiant heating systems to distribute heat or provide hot water. In winter, the GHP system provides geothermal energy to regulate the indoor temperature, while, in summer, it absorbs heat from rooms and restores it underground.

The GHP system uses electrical energy to realize space heating/cooling in target zones. The heat transfer depends on the flow rate and the supply temperature of the heat pump. Detailed operating principle of the GHP system is elaborated in Sarbu and Sebarchievici (2014).

2.2 Thermal Dynamic Models of GHP Systems

Consider community-level GHP systems in a certain district as shown in Figure 2. We denote $\mathcal{M}$ as the set of

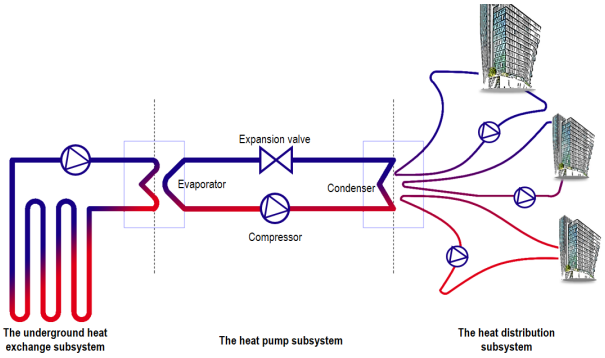

Fig. 1. One GHP system serving multiple buildings (take three buildings as an example).

GHPs for radiator heating/cooling. One heat pump provides geothermal energy or extracts heat through radiator pipes for buildings in set $\mathcal{K}_m, m \in \mathcal{M}$, each with a set of rooms/zones $\mathcal{R}_k, k \in \mathcal{K}_m$. Each building is modeled as a connected undirected graph $(\mathcal{R}_k, \mathcal{E}_k)$, where $\mathcal{R}_k$ represents the nodes collection of rooms in building $k \in \mathcal{K}_m, m \in \mathcal{M}$ and $\mathcal{E}_k \subseteq \mathcal{R}_k \times \mathcal{R}_k$ represents the edges collection. If room i is adjacent to room j in building k, there exists an edge (i, j) in the collection $\mathcal{E}_k$. $\mathcal{R}_k(i)$ is the collection of adjacent rooms for room i in building k.

For room $i \in \mathcal{R}_k$, we apply a second-order Resistance-Capacitance (RC) model for its thermal dynamics (more discussion on a simplified one is in Zhang et al. (2017)):

$$C_{ki}\dot{T}_{ki} = \frac{T_k^o - T_{ki}}{R_{ki}} + \sum_{j \in \mathcal{R}_k(i)} \frac{T_{kij} - T_{ki}}{R_{kij}} + \sum_{n_{ki}=1}^{N_{ki}} \frac{T_{n_{ki}} - T_{ki}}{R_{ar_{ki}}} + Q_{ki} \tag{1a}$$

$$C_{kij}\dot{T}_{kij} = \frac{T_{ki} - T_{kij}}{R_{kij}} + \frac{T_{kj} - T_{kij}}{R_{kij}} \tag{1b}$$

where C_{ki} denotes the thermal capacitance of the indoor air, C_{kij} denotes the thermal capacitance of the partition area of walls and windows, R_{ki} is the the thermal resistance in the partition area of walls and windows which separate room i and the outside environment, R_{kij}=R_{kji} is the thermal resistance in the partition area of walls and windows which separate room i and adjacent room j, $R_{ar_{ki}}$ is the thermal resistance between the radiator and the indoor air, T_{ki} is the indoor temperature of room i in building k, T_{kij} is the temperature of the seperating wall and window between room i and room j. Note that (i) the radiator pipe is divided into N_{ki} sections, and N_{ki} varies among different rooms, (ii) for each section, the entering water temperature is $T_{0_{ki}} = T_{s_m}$ and the leaving/terminal water temperature is $T_{N_{ki}}$, where T_{s_m} is a common factor for all buildings connected with the same heat pump $m \in \mathcal{M}$ in building set $\mathcal{K}_m$, where $T_{n_{ki}}$ denotes the water temperature in the nth section of the pipe in room i of building $k \in \mathcal{K}_m$, (iii) T_k^o is the outside temperature of building k and $Q_{ki} \geq 0$ indicates the heat disturbances from external sources (e.g., user activity, solar radiation and device operation).

Since the GHP system is expected to have a better tracking ability, for an individual building k, the thermal dynamic model of the radiator heating system is formulated by a high-order lumped element model:

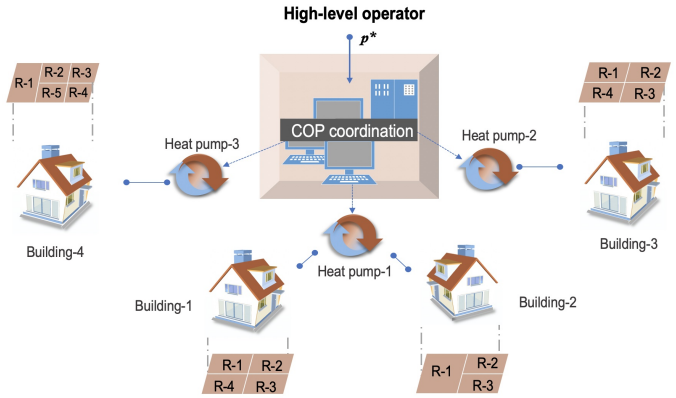

Fig. 2. Community-level GHP systems (take three heat pumps with four buildings as an example).

$$C_{n_{ki}}\dot{T}_{n_{ki}} = \frac{T_{ki}-T_{n_{ki}}}{R_{ar_{ki}}} + c_w q_{ki}(T_{n-1_{ki}} - T_{n_{ki}}) \quad (2)$$

where $k \in \mathcal{K}_m$, $i \in \mathcal{R}_k$, $n_{ki}=1,2,\cdots,N_{ki}$ $(n-1_{ki}=n_{ki}-1)$, $C_{n_{ki}}$ is the thermal capacitance of radiator pipe, c_w is the specific heat of the water, and q_{ki} is the water flow rate in radiator pipe for room i in building k. As for the nth section of the radiator pipe, the entering water temperature is $T_{n-1_{ki}}$, and the leaving water temperature is $T_{n_{ki}}$, all surrounded by room temperature T_{ki}. The term $c_w q_{ki}(T_{n-1_{ki}}-T_{n_{ki}})$ denotes the heat transferred in the nth section.

Remark 1. When the radiator heating/cooling system equipped with GHP system is off (q_{ki}=0), (1)-(2) asymptotically converges to an equilibrium point, only determined by disturbances T_k^o, Q_{ki}. When the radiator heating/cooling system equipped with GHP system is on, the asymptotic convergence property of (1)-(2) remains and the steady state is determined by disturbances T_k^o, Q_{ki} and control inputs q_{ki}, T_{s_m}. Since the key point is to design the dynamics of q_{ki}, T_{s_m} to drive (1)-(2) to the desired state set by users and administrators, we consider the steady-state problem, see derivation in Zhang et al. (2017).

Remark 2. Let $B_{ar_{ki}} = 1/R_{ar_{ki}}$, the heat loss in the water pipe can be summed as $H_{ki} = \sum_{n_{ki}=1}^{N_{ki}} B_{ar_{ki}}(T_{n_{ki}} - T_{ki}) = c_w q_{ki}(T_{s_m} - T_{N_{ki}})$, which is exactly the energy consumption of room i for heating/cooling. The terminal temperature is computed as $T_{N_{ki}} = (1-(\frac{c_w q_{ki}}{c_w q_{ki}+B_{ar_{ki}}})^{N_{ki}})T_{ki} + (\frac{c_w q_{ki}}{c_w q_{ki}+B_{ar_{ki}}})^{N_{ki}} T_{s_m}$. In steady state, the energy consumption is $H_{ki} = c_w q_{ki}[1-(\frac{c_w q_{ki}}{c_w q_{ki}+B_{ar_{ki}}})^{N_{ki}}](T_{s_m} - Z_{ki})$, where Z_{ki} is the steady-state temperature of T_{ki}, and let $u_{ki} = c_w q_{ki}[1-(\frac{c_w q_{ki}}{c_w q_{ki}+B_{ar_{ki}}})^{N_{ki}}](T_{s_m} - Z_{ki})$. In a heating mode (winter), $T_{s_m} > T_{ki}, T_{s_m} > Z_{ki}, \forall m, \forall k, \forall i$ hold; in a cooling mode (summer), $T_{s_m} < T_{ki}, T_{s_m} < Z_{ki}, \forall m, \forall k, \forall i$ hold. Once the mode is determined, the sign of $T_{s_m} - T_{ki}$ (or $T_{s_m} - Z_{ki}$) is confirmed.

3. SCENARIO I: ONE GHP SYSTEM SERVING MULTIPLE BUILDINGS

3.1 Problem Setup

For each building, the efficiency of the heat pump subsystem is determined by the Coefficient of Performance (COP), which is the ratio between the amount of useful cooling at the evaporator or useful heat extracted from the condenser and the energy usage of the compressor. A high COP value represents high efficiency, less electricity consumption and a cut down in energy costs. The COP can be approximately described as a linear function of T_{s_m}, i.e., $-a_m T_{s_m} + b_m$. Here a_m, b_m are positive coefficients, which can be obtained from the statistical data (Tahersima (2012)).

In this section, we consider multiple buildings sharing one GHP system. Since the power system structure is hierarchical, the ideal plan of GHP control should be included in the operation of higher-level power systems. Namely, the lower-level GHP system should track the given operating signal from the higher-level operator. Thus, the objectives here include regulating the indoor temperature to be close to the set point T_{ki}^{set} in each room within a desired range, promoting energy efficiency of the GHP by maximizing its COP (minimizing the supply temperature), and improving the ability to track the given nominal value of electrical power consumption p_b^*.

The temperature of each room is regulated by adjusting the control inputs of flow rate q_{ki} and the supply temperature T_{s_m} of the heat pump. *For simplicity we drop the subscript m in this section, since only one GHP is considered.* To make the formulation clear, we only focus on the steady-state performance. The steady-state optimization problem with operational constraints is:

$$\min_{Z_{ki},u_{ki},T_s} \frac{\phi_a}{2}\sum_{k\in\mathcal{K}}\sum_{i\in\mathcal{R}_k}(Z_{ki}-T_{ki}^{set})^2 + \frac{\phi_c}{2}(T_s-\underline{T_s})^2 + \frac{\phi_b}{2}(\sum_{k\in\mathcal{K}}\sum_{i\in\mathcal{R}_k} u_{ki} - p_b^*(b-aT_s))^2 \quad (3a)$$

$$\text{s. t. } \frac{T_k^o - Z_{ki}}{R_{ki}} + \sum_{j\in\mathcal{R}_k(i)}\frac{Z_{kj}-Z_{ki}}{2R_{kij}} + u_{ki} + Q_{ki} = 0 \quad (3b)$$

$$\underline{T_{ki}} \leqslant Z_{ki} \leqslant \overline{T_{ki}} \quad (3c)$$

$$\underline{T_s} \leqslant T_s \leqslant \overline{T_s} \quad (3d)$$

$$0 \leqslant u_{ki} \leqslant c_w q_{ki}^{max}[1-(\frac{c_w q_{ki}^{max}}{c_w q_{ki}^{max}+B_{ar_{ki}}})^{N_{ki}}](T_s - Z_{ki}) \quad (3e)$$

where $k \in \mathcal{K}$ and $i \in \mathcal{R}_k$, ϕ_a, ϕ_b and ϕ_c are non-negative weight coefficients, ϕ_a represents the priority of user comfort, ϕ_c represents the priority of promoting energy efficiency, and ϕ_b represents the priority of tracking the given p_b^*. The term $\sum_{k\in\mathcal{K}_m}\sum_{i\in\mathcal{R}_k} u_{ki}/(-aT_s+b)$ is equivalent to the electrical power consumption in the GHP system, where $\sum_{k\in\mathcal{K}_m}\sum_{i\in\mathcal{R}_k} u_{ki}$ denotes the total heat transferred from the heat pump to the water in radiator pipes of buildings connected to pump m. $Z_{ki} \in [\underline{T_{ki}}, \overline{T_{ki}}]$, $q_{ki} \in [0, q_{ki}^{max}]$, $T_s \in [\underline{T_s}, \overline{T_s}]$. Through analyses in the monotonicity of u_{ki}, we can prove that u_{ki} is a monotonic increasing function of the variable q_{ki}, which results in (3e). Obviously, this steady-state optimization problem is convex. We assume (3) is feasible and satisfied with the Slater's condition (Boyd and Vandenberghe (2004)).

3.2 A Distributed Controller

Compared with centralized algorithms, distributed algorithms are involved with fewer privacy issues. Also, they

are easy to plug and play for large-scale networks. Moreover, they can be implemented without measuring the outdoor temperature T_k^o and the indoor heat gain Q_{ki} in every room for each building, as will be shown later. So we develop a real-time distributed controller to regulate (1)-(2) to a steady state which is the optimal solution to (3). We consider the heating mode case (the cooling mode case is similar).

To solve the optimization problem (3), we apply the same design procedure as in Zhang et al. (2017), i.e., a modified primal-dual gradient method, to get

$$\begin{aligned}\dot{Z}_{ki} =& -k_{Z_{ki}}(\frac{\partial L}{\partial Z_{ki}}) = k_{Z_{ki}}[\phi_a(T_{ki}^{set}-Z_{ki})\\ &+\zeta_{ki}(\frac{1}{R_{ki}}+\sum_{j\in R_k(i)}\frac{1}{2R_{kij}})-\sum_{j\in\mathcal{R}_k(i),\forall i}\frac{\zeta_{kj}}{2R_{kij}}+\delta_{ki}^- -\delta_{ki}^+\\ &-\mu_{ki}^+ c_w q_{ki}^{max}[1-\big(\frac{c_w q_{ki}^{max}}{c_w q_{ki}^{max}+B_{ar_{ki}}}\big)^{N_{ki}}]] \qquad (4a)\\ \dot{u}_{ki} =& -k_{u_{ki}}(\frac{\partial L}{\partial u_{ki}}+k_{eu_{ki}}(u_{ki}-\hat{u}_{ki}))\\ =& \quad k_{u_{ki}}[\phi_b\big(p_b^*(b-aT_s)-\sum_{k\in\mathcal{K}}\sum_{i\in\mathcal{R}_k}u_{ki}\big)-\zeta_{ki}\\ &+\mu_{ki}^- -\mu_{ki}^+ +k_{eu_{ki}}(\hat{u}_{ki}-u_{ki})] \qquad (4b)\\ \dot{\hat{u}}_{ki} =& \quad \hat{k}_{eu_{ki}}(u_{ki}-\hat{u}_{ki}) \qquad (4c)\\ \dot{T}_s =& -k_{T_s}(\frac{\partial L}{\partial T_s}) = k_{T_s}[\phi_c(\underline{T_s}-T_s)\\ &+ap_b^*\phi_b\big(p_b^*(b-aT_s)-\sum_{k\in\mathcal{K}}\sum_{i\in\mathcal{R}_k}u_{ki}\big)-\varepsilon^+ +\varepsilon^-\\ &+\sum_{k\in\mathcal{K}}\sum_{i\in\mathcal{R}_k}\mu_{ki}^+ c_w q_{ki}^{max}[1-(\frac{c_w q_{ki}^{max}}{c_w q_{ki}^{max}+B_{ar_{ki}}})^{N_{ki}}]] \qquad (4d)\\ \dot{\zeta}_{ki} =& k_{\zeta_{ki}}(\frac{\partial L}{\partial \zeta_{ki}})\\ =& k_{\zeta_{ki}}[\frac{T_k^o-Z_{ki}}{R_{ki}}+\sum_{j\in\mathcal{R}_k(i)}\frac{Z_{kj}-Z_{ki}}{2R_{kij}}+u_{ki}+Q_{ki}] \qquad (4e)\\ \dot{\delta}_{ki}^- =& k_{\delta_{ki}^-}(\frac{\partial L}{\partial \delta_{ki}^-})_{\delta_{ki}^-}^+ = k_{\delta_{ki}^-}(\underline{T_{ki}}-Z_{ki})_{\delta_{ki}^-}^+ \qquad (4f)\\ \dot{\delta}_{ki}^+ =& k_{\delta_{ki}^+}(\frac{\partial L}{\partial \delta_{ki}^+})_{\delta_{ki}^+}^+ = k_{\delta_{ki}^+}(Z_{ki}-\overline{T_{ki}})_{\delta_{ki}^+}^+ \qquad (4g)\\ \dot{\varepsilon}^- =& k_{\varepsilon^-}(\frac{\partial L}{\partial \varepsilon^-})_{\varepsilon^-}^+ = k_{\varepsilon^-}(\underline{T_s}-T_s)_{\varepsilon^-}^+ \qquad (4h)\\ \dot{\varepsilon}^+ =& k_{\varepsilon^+}(\frac{\partial L}{\partial \varepsilon^+})_{\varepsilon^+}^+ = k_{\varepsilon^+}(T_s-\overline{T_s})_{\varepsilon^+}^+ \qquad (4i)\\ \dot{\mu}_{ki}^- =& k_{\mu_{ki}^-}(\frac{\partial L}{\partial \mu_{ki}^-})_{\mu_{ki}^-}^+ = k_{\mu_{ki}^-}(-u_{ki})_{\mu_{ki}^-}^+ \qquad (4j)\\ \dot{\mu}_{ki}^+ =& k_{\mu_{ki}^+}(\frac{\partial L}{\partial \mu_{ki}^+})_{\mu_{ki}^+}^+ = k_{\mu_{ki}^+}(u_{ki}-c_w q_{ki}^{max}(T_s\\ &-Z_{ki})[1-(\frac{c_w {q_{ki}}^{max}}{c_w {q_{ki}}^{max}+B_{ar_{ki}}})^{N_{ki}}])_{\mu_{ki}^+}^+ \qquad (4k)\end{aligned}$$

where L is the Lagrangian of (3), $k\in\mathcal{K}$, $i\in\mathcal{R}_k$, $\zeta_{ki},\delta_{ki}^-,\delta_{ki}^+,\varepsilon^-,\varepsilon^+,\mu_{ki}^-,\mu_{ki}^+$ denote the Lagrange multipliers/dual variables for constraints (3b)-(3e), $k_{Z_{ki}}$, $k_{u_{ki}}$, $k_{eu_{ki}}$, $\hat{k}_{eu_{ki}}$, k_{T_s}, $k_{\zeta_{ki}}$, $k_{\delta_{ki}^-}$, $k_{\delta_{ki}^+}$, k_{ε^-}, k_{ε^+}, $k_{\mu_{ki}^-}$, $k_{\mu_{ki}^+}$ are positive scalars representing the controller gains, and the operator $(h(y))_x^+$ means positive projection of functions as

$$(h(y))_x^+ = \begin{cases} h(y) & \text{if } x>0\\ \max(0,h(y)) & \text{if } x=0\end{cases}.$$

Auxiliary states $\hat{u}_{ki}$ is introduced to decrease oscillations in transient periods. Note that T_{ki} has dynamics given by (1), which cannot be designed. So T_{ki} has been substituted by Z_{ki} in (3), i.e., $Z_{ki}, k\in\mathcal{K}, i\in\mathcal{R}_k$ are ancillary state variables. According to Zhang et al. (2015) and Feijer and Paganini (2010), (4) asymptotically converges to an equilibrium point, which is the optimal solution of (3) due to the convexity. Now with the control input to (1)-(2) as

$$\begin{aligned}\dot{q}_{ki} =& k_{q_{ki}}(u_{ki}-c_w q_{ki}(T_s-Z_{ki})[1-(\frac{c_w q_{ki}}{c_w q_{ki}+B_{ar_{ki}}})^{N_{ki}}]\\ &+k_{eq_{ki}}(\hat{q}_{ki}-q_{ki})) \qquad (5a)\\ \dot{\hat{q}}_{ki} =& \hat{k}_{eq_{ki}}(q_{ki}-\hat{q}_{ki}) \qquad (5b)\end{aligned}$$

where $k_{q_{ki}}, k_{eq_{ki}}, \hat{k}_{eq_{ki}}$ are controller gains and $\hat{q}_{ki}$ is introduced to improve the transient performance, (1)-(2) can be regulated to a steady state that is the optimum to (3).

Theorem 1. Given constant/slow-varying T_k^o, Q_{ki}, the trajectory of the controlled system (1)-(2) and (4)-(5) asymptotically converges to an equilibrium point at which T_{ki}, u_{ki}, T_s of the equilibrium point is the optimal solution of (3) (u_{ki}=$c_w q_{ki}[1-(\frac{c_w q_{ki}}{c_w q_{ki}+B_{ar_{ki}}})^{N_{ki}}](T_s-Z_{ki})$).

Proof. Under (5), after state transformation from u_{ki} to q_{ki}, the resulting equilibrium point is the optimal solution of (3). On the other hand, the trajectory of the system (1)-(2) and (4)-(5) also asymptotically converges to an equilibrium point, due to the cascade nature, i.e., (4)→(5)→(1)-(2). It is clear that the equilibrium point of (1)-(2) is uniquely determined by the inputs $T_k^o, Q_{ki}, q_{ki}, T_s$ where q_{ki} is given by (5). So we have $T_{ki}=Z_{ki}$ (here T_{ki} is a state given by (1)-(2)) when the system reaches steady state, which completes the proof.

In Equation (4e), the disturbances T_k^o, Q_{ki} appear. Similar to Zhang et al. (2015), the variable $\tilde{\zeta}_{ki}=\frac{\zeta_{ki}}{k_{\zeta_{ki}}}-C_{ki}T_{ki}$ can be introduced to make the scheme implemented more practically, which does not require measuring the external disturbances:

$$\begin{aligned}\dot{\tilde{\zeta}}_{ki} =& \frac{T_{ki}-Z_{ki}}{R_{ki}}+\sum_{j\in\mathcal{R}_k(i)}\frac{2T_{ki}-Z_{ki}+Z_{kj}-2T_{kij}}{2R_{kij}}\\ &+u_{ki}-\sum_{n_{ki}=1}^{N_{ki}}\frac{T_{n_{ki}}-T_{ki}}{R_{ar_{ki}}},\ k\in\mathcal{K}, i\in\mathcal{R}_k. \qquad (6)\end{aligned}$$

In addition, $k_{\zeta_{ki}}(\tilde{\zeta}_{ki}+C_{ki}T_{ki})$ is introduced to (4a) and (4b) to replace ζ_{ki}. Then, the overall control scheme (4a)-(4d), (4f)-(4k) and (5)-(6) can be implemented in a fully distributed manner, which inherits from the algorithm (4).

Implementation. In the designed controller, C_{ki}, $C_{n_{ki}}$, R_{kij}, $R_{ar_{ki}}$, R_{ki}, q_{ki}^{max}, a, b, $\underline{T_s}$, $\overline{T_s}$ are building parameters, ϕ_a,ϕ_c,ϕ_b are set by users or administrators, p^* is the given nominal point from the higher-level operator. The scheme is distributed and can be implemented as follows. Given $C_{ki}, C_{n_{ki}}, R_{kij}, R_{ar_{ki}}, R_{ki}, q_{ki}^{max}, \phi_a, c_w$, the information about $[\underline{T_{ki}}, \overline{T_{ki}}]$, T_{ki}^{set} is collected from users, the temperature $T_{ki}, T_{kj}, T_{n_{ki}}$ is measured, feedback signals $Z_{kj}-2T_{kij}, k_{\zeta_{kj}}(\tilde{\zeta}_{kj}+C_{kj}T_{kj})$ from the neighboring zones and $T_s, \phi_b(p_b^*(b-aT_s)-\sum_{k\in\mathcal{K}}\sum_{i\in\mathcal{R}_k}u_{ki})$ from

the heat pump are sent to the controller in order to update $Z_{ki}, u_{ki}, \hat{u}_{ki}, k_{\zeta_{ki}}(\tilde{\zeta}_{ki}+C_{ki}T_{ki}), \delta^+_{ki}, \delta^-_{ki}, \mu^+_{ki}, \mu^-_{ki}, q_{ki}$. On the other hand, given $\phi_c, \phi_b, p^*, a, b, [\underline{T_s}, \overline{T_s}]$, the compressor receives the feedback signals $u_{ki}, \mu^+_{ki} c_w q^{max}_{ki}[1 - (\frac{c_w q^{max}_{ki}}{c_w q^{max}_{ki}+B_{ar_{ki}}})^{N_{ki}}]$ from each zone, updates $T_s, \sigma^+_{ki}, \sigma^-_{ki}$,and then renew $T_s, \phi_b(p^*_b(b-aT_s) - \sum_{k\in\mathcal{K}}\sum_{i\in\mathcal{R}_k} u_{ki})$.

4. SCENARIO II: COMMUNITY-LEVEL COORDINATION OF MULTIPLE GHP SYSTEMS

4.1 Problem Setup

In this scenario, we consider the community-level GHP systems in neighboring areas. The objective is similar to Section 3 except for the part about COP. To reduce the complexity of the problem, we seek a homogeneous COP value in the optimization problem and try the best to maximize it. By doing so, the control scheme proposed in Section 3 can be naturally applied. Similarly, we only focus on steady-state performance. The target optimization problem is then designed as follow:

$$\min_{Z_{ki},u_{ki},T_{s_m},\lambda} \frac{\phi_a}{2}\sum_{k\in\mathcal{K}}\sum_{i\in\mathcal{R}_k}(Z_{ki}-T^{set}_{ki})^2 + \frac{\psi}{2}(\overline{\lambda}-\lambda)^2 + \frac{\phi_b}{2}(\sum_{k\in\mathcal{K}}\sum_{i\in\mathcal{R}_k} u_{ki} - p^*_b\lambda)^2 \tag{7a}$$

$$\text{s.t.}\ \frac{T^o_k - Z_{ki}}{R_{ki}} + \sum_{j\in\mathcal{R}_k(i)}\frac{Z_{kj}-Z_{ki}}{2R_{kij}} + u_{ki} + Q_{ki} = 0 \tag{7b}$$

$$-a_m T_{s_m} + b_m = \lambda \tag{7c}$$

$$\underline{T_{ki}} \leqslant Z_{ki} \leqslant \overline{T_{ki}} \tag{7d}$$

$$\underline{T_{s_m}} \leqslant T_{s_m} \leqslant \overline{T_{s_m}} \tag{7e}$$

$$0 \leqslant u_{ki} \leqslant c_w q^{max}_{ki}[1 - (\frac{c_w q^{max}_{ki}}{c_w q^{max}_{ki}+B_{ar_{ki}}})^{N_{ki}}](T_{s_m} - Z_{ki}), \quad \forall k \in \mathcal{K}_m \tag{7f}$$

where $k \in \mathcal{K} = \cup_{m\in\mathcal{M}}\mathcal{K}_m$, $i \in \mathcal{R}_k$, $m \in \mathcal{M}$, ψ is a positive weight coefficient representing the priority of optimizing the common COP value λ for all heat pumps in the district, and $\overline{\lambda} = \min_m\{-a_m\underline{T_{s_m}} + b_m\}$. All GHP systems adopt the same COP value $\overline{\lambda}$ to realize the tracking goal.

4.2 A Distributed Algorithm

Similar as Section 3.2, we take the heating mode case as an example. As shown before, according to a modified primal-dual gradient method, problem (7) is solved via:

$$\dot{Z}_{ki} = k_{Z_{ki}}[\phi_a(T^{set}_{ki} - Z_{ki}) + \zeta_{ki}(\frac{1}{R_{ki}} + \sum_{j\in\mathcal{R}_k(i)}\frac{1}{2R_{kij}}) - \sum_{j\in\mathcal{R}_k(i),\forall i}\frac{\zeta_{kj}}{2R_{kij}} + \delta^-_{ki} - \delta^+_{ki} - \mu^+_{ki}c_w q^{max}_{ki}[1 - \big(\frac{c_w q^{max}_{ki}}{c_w q^{max}_{ki}+B_{ar_{ki}}}\big)^{N_{ki}}]] \tag{8a}$$

$$\dot{u}_{ki} = k_{u_{ki}}[\phi_b(p^*_b\lambda - \sum_{k\in\mathcal{K}}\sum_{i\in\mathcal{R}_k} u_{ki}) - \zeta_{ki} + \mu^-_{ki} - \mu^+_{ki} + k_{eu_{ki}}(\hat{u}_{ki} - u_{ki})] \tag{8b}$$

$$\dot{\hat{u}}_{ki} = \hat{k}_{eu_{ki}}(u_{ki} - \hat{u}_{ki}) \tag{8c}$$

$$\dot{T}_{s_m} = k_{T_{s_m}}[-\varepsilon^+_m + \varepsilon^-_m + a_m\eta_m + \sum_{k\in\mathcal{K}_m}\sum_{i\in\mathcal{R}_k}\mu^+_{ki}c_w q^{max}_{ki}[1 - (\frac{c_w q^{max}_{ki}}{c_w q^{max}_{ki}+B_{ar_{ki}}})^{N_{ki}}] + k_{eT_{s_m}}(\hat{T}_{s_m} - T_{s_m})] \tag{8d}$$

$$\dot{\hat{T}}_{s_m} = \hat{k}_{eT_{s_m}}(T_{s_m} - \hat{T}_{s_m}) \tag{8e}$$

$$\dot{\lambda} = k_\lambda[\psi(\overline{\lambda}-\lambda) + \phi_b p^*_b(\sum_{k\in\mathcal{K}}\sum_{i\in\mathcal{R}_k} u_{ki} - p^*_b\lambda) + \sum_{m\in\mathcal{M}}\eta_m] \tag{8f}$$

$$\dot{\zeta}_{ki} = k_{\zeta_{ki}}[\frac{T^o_k - Z_{ki}}{R_{ki}} + \sum_{j\in\mathcal{R}_k(i)}\frac{Z_{kj}-Z_{ki}}{2R_{kij}} + u_{ki} + Q_{ki}] \tag{8g}$$

$$\dot{\eta}_m = k_{\eta_m}(-a_m T_{s_m} + b_m - \lambda) \tag{8h}$$

$$\dot{\delta}^-_{ki} = k_{\delta^-_{ki}}(\underline{T_{ki}} - Z_{ki})^+_{\delta^-_{ki}}, \quad \dot{\delta}^+_{ki} = k_{\delta^+_{ki}}(Z_{ki} - \overline{T_{ki}})^+_{\delta^+_{ki}} \tag{8i}$$

$$\dot{\varepsilon}^-_m = k_{\varepsilon^-_m}(\underline{T_{s_m}} - T_{s_m})^+_{\varepsilon^-_m}, \quad \dot{\varepsilon}^+_m = k_{\varepsilon^+_m}(T_{s_m} - \overline{T_{s_m}})^+_{\varepsilon^+_m} \tag{8j}$$

$$\dot{\mu}^-_{ki} = k_{\mu^-_{ki}}(-u_{ki})^+_{\mu^-_{ki}},$$

$$\dot{\mu}^+_{ki} = k_{\mu^+_{ki}}(u_{ki} - c_w q^{max}_{ki}[1 - (\frac{c_w q^{max}_{ki}}{c_w q^{max}_{ki}+B_{ar_{ki}}})^{N_{ki}}](T_{s_m} - Z_{ki}))^+_{\mu^+_{ki}} \tag{8k}$$

where $k \in \mathcal{K}, i \in \mathcal{R}_k, m \in \mathcal{M}$, and the variables and gains are defined in a similar way as in Section 3.2.

Theorem 2. Given constant/slow-varying T^o_k, Q_{ki}, the trajectory of the system (1)-(2), (5) and (8) asymptotically converges to an equilibrium point at which $T_{ki}, u_{ki}, T_{s_m}, \lambda$ of this point is the optimal solution of (7) (u_{ki}=$c_w q_{ki}[1 - (\frac{c_w q_{ki}}{c_w q_{ki}+B_{ar_{ki}}})^{N_{ki}}](T_{s_m} - Z_{ki})$).

Proof. The proof is similar to that of Theorem 1, and thus, is omitted for brevity.

In Equation (8g), the disturbances T^o_k, Q_{ki} appear. Using the method in Section 3.2, $\tilde{\zeta}_{ki} = \frac{\zeta_{ki}}{k_{\zeta_{ki}}} - C_{ki}T_{ki}$ with dynamics (6) can be introduced to eliminate the external disturbance terms. Additionally, ζ_{ki} is substituted by $k_{\zeta_{ki}}(\tilde{\zeta}_{ki}+C_{ki}T_{ki})$ in (8a)-(8b). Now the designed control scheme (8a)-(8f), (8h)-(8k) and (5)-(6) can be implemented in a fully distributed manner, which inherits from the distributed optimization algorithm (8).

Implementation. By sending building and coordinator information to the control center, the distributed scheme can be implemented in the community-level application as follows. Given $C_{ki}, C_{n_{ki}}, R_{kij}, R_{ar_{ki}}, R_{ki}, q^{max}_{ki}, \phi_a, c_w$, the information about $[\underline{T_{ki}}, \overline{T_{ki}}]$, T^{set}_{ki} is collected from users, the temperature $T_{ki}, T_{kj}, T_{n_{ki}}$ is measured, feedback signals $Z_{kj} - 2T_{kij}, k_{\zeta_{kj}}(\tilde{\zeta}_{kj} + C_{kj}T_{kj})$ from the neighboring zones, $\lambda, \phi_b p^*(\sum_{k\in\mathcal{K}}\sum_{i\in\mathcal{R}_k} u_{ki} - p^*_b\lambda)$ from the coordinator are sent to the controller in order to update $Z_{ki}, u_{ki}, \hat{u}_{ki}, k_{\zeta_{ki}}(\tilde{\zeta}_{ki}+C_{ki}T_{ki}), \delta^+_{ki}, \delta^-_{ki}, \mu^+_{ki}, \mu^-_{ki}, q_{ki}$. On the other hand, given $\psi, \phi_b, p^*, a_m, b_m, [\underline{T_{s_m}}, \overline{T_{s_m}}]$, the coordinator receives the feedback signals $u_{ki}, \mu^+_{ki}c_w q^{max}_{ki}[1 - (\frac{c_w q^{max}_{ki}}{c_w q^{max}_{ki}+B_{ar_{ki}}})^{N_{ki}}]$ from buildings, updates λ, η_m, and then each heat pump updates $T_{s_m}, \hat{T}_{s_m}, \varepsilon^+_{ki}, \varepsilon^-_{ki}$, and then renew $\lambda, \phi_b p^*(\sum_{k\in\mathcal{K}}\sum_{i\in\mathcal{R}_k} u_{ki} - p^*_b\lambda)$.

5. CASE STUDY

Two numerical examples are presented for scenarios stated in Section 3 and Section 4 respectively. For scenario

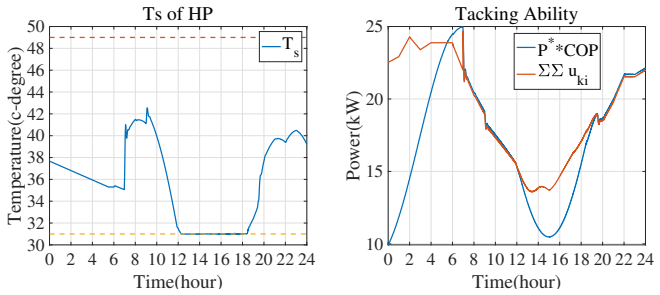

Fig. 3. Supply temperature (the left one) and tracking ability (the right one) of the system in scenario I.

I, as shown in Figure 1, the configuration is three buildings sharing one GHP systems. For scenario II, as shown in Figure 2, the configuration is three GHP systems serving four buildings. Only the heating mode is implemented in both scenarios, while the cooling mode is similar. In simulation, T_k^o, Q_{ki} are from Zhang et al. (2017), other parameters: $C_{ki} = 6\text{kJ/°C}, C_{n_{ki}} = 0.33\text{kJ/°C}, R_{kij}^L = 11.5\text{°C/kW}, R_{kij}^S = 23\text{°C/kW}, R_{ar_{ki}} = 9\text{°C/kW}, R_{ki} = 15\text{°C/kW}, c_w = 4.186\text{kJ/kg/°C}, q_{ki}^{max} = 0.1\text{kg/s}, [\underline{T_{ki}}, \overline{T_{ki}}] = [0.95T_{ki}^{set}, 1.05T_{ki}^{set}], [\underline{T_s}, \overline{T_s}] = [31, 49]\text{°C}, [\underline{T_{s_1}}, \overline{T_{s_1}}] = [36, 49]\text{°C}, [\underline{T_{s_2}}, \overline{T_{s_2}}] = [30, 40]\text{°C}, [\underline{T_{s_3}}, \overline{T_{s_3}}] = [30, 45]\text{°C}, a = a_2 = 0.11/\text{°C}, a_1 = 0.1/\text{°C}, a_3 = 0.12/\text{°C}, b = 8.4, b_1 = 8.6, b_2 = 8, b_3 = 8.5, k_{Z_{ki}} = 0.25, k_{u_{ki}} = k_{T_{s_2}} = k_{T_{s_3}} = k_\lambda = k_{q_{ki}} = 0.9, k_{T_s} = k_{T_{s_1}} = k_{\zeta_{ki}} = 0.5, k_{\eta_m} = k_{\delta_{ki}^+} = k_{\delta_{ki}^-} = k_{\varepsilon^+} = k_{\varepsilon^-} = k_{\varepsilon_m^+} = k_{\varepsilon_m^-} = k_{\mu_{ki}^+} = k_{\mu_{ki}^-} = \hat{k}_{eT_{sm}} = \hat{k}_{eu_{ki}} = \hat{k}_{eq_{ki}} = 1, k_{eu_{ki}} = k_{eq_{ki}} = k_{eT_{s_m}} = 2$. Note that R_{kij}^L is the R_{kij} value for large rooms, R_{kij}^S is the R_{kij} value for other rooms. In case I, the weight coefficients are $\phi_a = 3, \phi_b = \phi_c = 0$ before 7h and $\phi_b = 10, \phi_c = 0.01$ thereafter. In case II, the weight coefficients are $\phi_a = 0.8, \psi = \phi_b = 0$ before 7h and $\phi_b = 3, \psi = 3$ thereafter. As for the given nominal point of electrical power consumption p^*, we assume it is a sine curve. To test the tracking ability, the designed systems have to track a signal, about ±15% of base energy consumption from a high-level operator in both scenarios.

The simulation results for the first scenario are shown in Figures 3 and 4. It reveals that when $\phi_c = 0$, the tendency of T_{ki} closely follows the changes of T_{ki}^{set}, which means the designed control scheme works well in regulating temperatures before considering tracking the given nominal electrical power consumption. The results show that changes of the temperatures of the adjacent rooms will result in thermal fluctuations, but that only causes little impact. The tracking ability of the control scheme is shown in Figure 3. After considering the tracking ability, the designed control scheme can still keep good performance on the user comfort. From 12h to 18h, the system cannot work well to track the given nominal p_b^*. The reason lies in that the supply temperature has reached the lower limit with the highest COP value. Also, the user comfort from 12h to 18h is sacrificed.

Simulation results for scenario II are demonstrated in Figures 5 and 6. Temperature damping from T_{ki}^{set} after changing ϕ_b, ψ are much higher than that before 7h. Results show that the performance of each heat pump is closely linked to the range of its supply temperature $[\underline{T_{s_m}}, \overline{T_{s_m}}]$: T_{s_m} can reach its lower bound if needed for further energy reduction. Moreover, if the ability of tracking p_b^* is taken into consideration, the user comfort will be sacrificed to some extent as well. From 19h to 22h, since the given p_b^* is too high, the system has to improve the supply temperature to realize the tracking goal. Simulation results of the two scenarios show that by changing the weight coefficient ϕ_a, ϕ_b, ϕ_c and ψ, users can realize the goal of improving comfort and achieving energy conservation in a distributed manner. Besides, the designed control schemes can track a given nominal point of electrical power consumption.

6. CONCLUSION AND FUTURE WORK

In this paper, a real-time distributed control scheme have been designed to balance the user comfort, efficiency of heat pumps and the ability to track the nominal power consumption in the thermal and energy management with GHP systems. Specially, high-order thermal dynamic models for the radiator heating systems in buildings is considered to make the control scheme more realistic and accurate. In the future, research on the sensor-based parameter identification of thermal dynamic models will be studied. Also, an aggregation-disaggregation framework of the community-level GHP system management (with heterogeneous heat distribution subsystems) will be formulated, which is an extension of this work.

REFERENCES

Afram, A. and Janabi-Sharifi, F. (2016). Effects of deadband and set-point settings of on/off controllers on the energy consumption and equipment switching frequency of a residential hvac system. *Journal of Process Control*, 47, 161–174.

Al Shibli, M. and Mathew, B. (2019). Artificial intelligent machine learning and big data mining of desert geothermal heat pump: Analysis, design and control.

Amara, F., Agbossou, K., Cardenas, A., Dubé, Y., and Kelouwani, S. (2015). Comparison and simulation of building thermal models for effective energy management. *Smart Grid and renewable energy*, 6(04), 95.

Boyd, S. and Vandenberghe, L. (2004). *Convex optimization*. Cambridge university press.

Feijer, D. and Paganini, F. (2010). Stability of primal–dual gradient dynamics and applications to network optimization. *Automatica*, 46(12), 1974–1981.

Informative, E. (2019). Saving money with geothermal heat pumps. `https://energyinformative.org`. Accessed Octorber 24, 2019.

Joe, J. and Karava, P. (2019). A model predictive control strategy to optimize the performance of radiant floor heating and cooling systems in office buildings. *Applied Energy*, 245, 65–77.

Madani, H., Claesson, J., and Lundqvist, P. (2011). Capacity control in ground source heat pump systems part ii: Comparative analysis between on/off controlled and variable capacity systems. *International journal of refrigeration*, 34(8), 1934–1942.

Maivel, M. and Kurnitski, J. (2014). Low temperature radiator heating distribution and emission efficiency in residential buildings. *Energy and Buildings*, 69, 224–236.

Omer, A.M. (2008). Ground-source heat pumps systems and applications. *Renewable and sustainable energy reviews*, 12(2), 344–371.

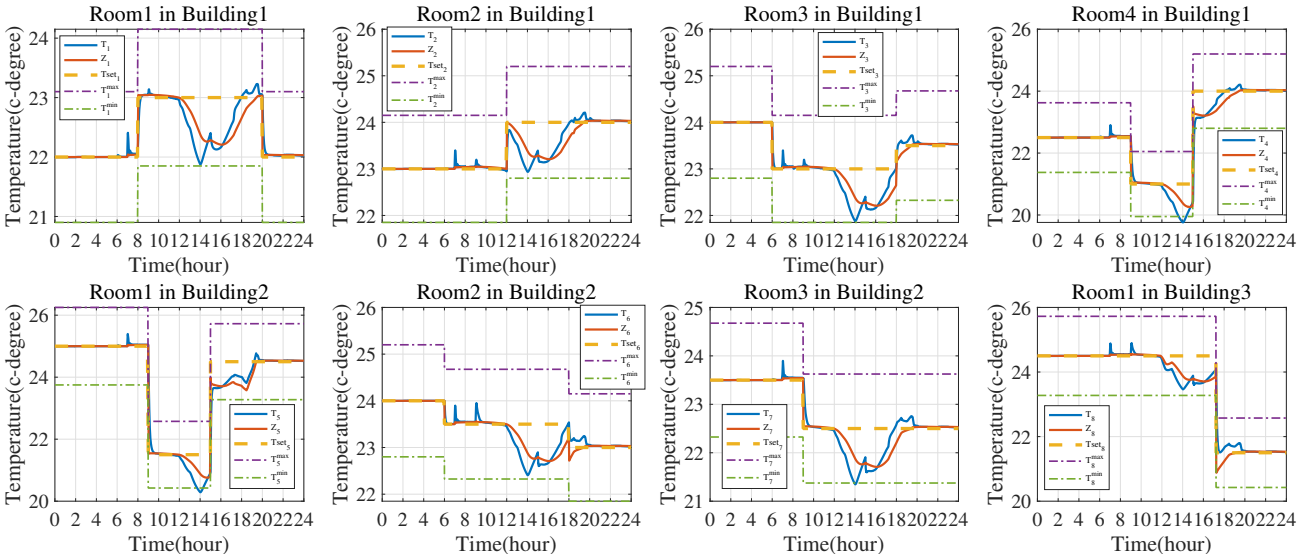

Fig. 4. Partial temperature results in scenario I.

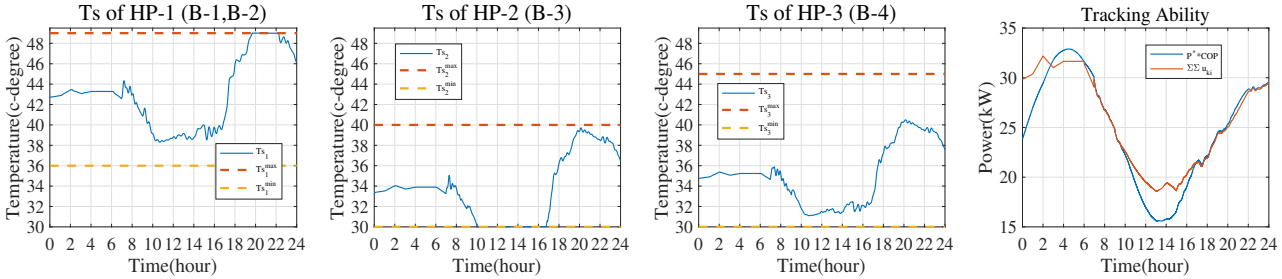

Fig. 5. Supply temperature and tracking ability of the system in scenario II.

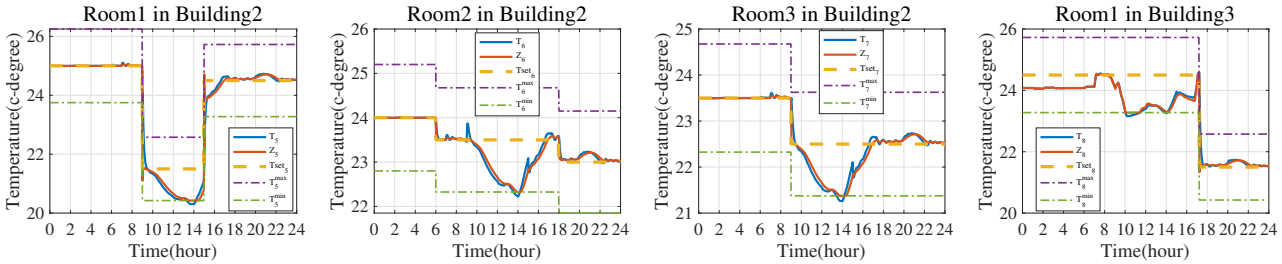

Fig. 6. Partial temperature results in scenario II.

Pérez-Lombard, L., Ortiz, J., and Pout, C. (2008). A review on buildings energy consumption information. *Energy and buildings*, 40(3), 394–398.

Sarbu, I. and Sebarchievici, C. (2014). General review of ground-source heat pump systems for heating and cooling of buildings. *Energy and buildings*, 70, 441–454.

Self, S.J., Reddy, B.V., and Rosen, M.A. (2013). Geothermal heat pump systems: Status review and comparison with other heating options. *Applied Energy*, 101(1), 341–348.

Tahersima, F. (2012). *An integrated control system for heating and indoor climate applications*. Ph.D. thesis, Ph. D. Thesis.

Tahersima, F., Stoustrup, J., and Rasmussen, H. (2011). Optimal power consumption in a central heating system with geothermal heat pump. *IFAC Proceedings Volumes*, 44(1), 3102–3107.

Wen, J.T. and Mishra, S. (2018). Intelligent building control systems: A survey of modern building control and sensing strategies (advances in industrial control) 2018 edition. *ISBN-13*, 978–3319684611.

Zhang, X., Papachristodoulou, A., and Li, N. (2015). Distributed optimal steady-state control using reverse-and forward-engineering. In *2015 54th IEEE Conference on Decision and Control (CDC)*, 5257–5264. IEEE.

Zhang, X., Shi, W., Hu, Q., Yan, B., Malkawi, A., and Li, N. (2017). Distributed temperature control via geothermal heat pump systems in energy efficient buildings. In *2017 American Control Conference (ACC)*, 754–760. IEEE.